Suppression pattern of neutral pions at high transverse momentum in Au+Au collisions at $\sqrt{s_{NN}}$=200 GeV and constraints on medium transport coefficients

A. Adare,[8] S. Afanasiev,[22] C. Aidala,[9] N.N. Ajitanand,[49] Y. Akiba,[43,44] H. Al-Bataineh,[38] J. Alexander,[49] A. Al-Jamel,[38] K. Aoki,[28,43] L. Aphecetche,[51] R. Armendariz,[38] S.H. Aronson,[3] J. Asai,[44] E.T. Atomssa,[29] R. Averbeck,[50] T.C. Awes,[39] B. Azmoun,[3] V. Babintsev,[18] G. Baksay,[14] L. Baksay,[14] A. Baldisseri,[11] K.N. Barish,[4] P.D. Barnes,[31] B. Bassalleck,[37] S. Bathe,[4] S. Batsouli,[9,39] V. Baublis,[42] F. Bauer,[4] A. Bazilevsky,[3] S. Belikov,[3,21,*] R. Bennett,[50] Y. Berdnikov,[46] A.A. Bickley,[8] M.T. Bjorndal,[9] J.G. Boissevain,[31] H. Borel,[11] K. Boyle,[50] M.L. Brooks,[31] D.S. Brown,[38] D. Bucher,[34] H. Buesching,[3] V. Bumazhnov,[18] G. Bunce,[3,44] J.M. Burward-Hoy,[31] S. Butsyk,[31,50] S. Campbell,[50] J.-S. Chai,[23] B.S. Chang,[58] J.-L. Charvet,[11] S. Chernichenko,[18] J. Chiba,[24] C.Y. Chi,[9] M. Chiu,[9,19] I.J. Choi,[58] T. Chujo,[55] P. Chung,[49] A. Churyn,[18] V. Cianciolo,[39] C.R. Cleven,[16] Y. Cobigo,[11] B.A. Cole,[9] M.P. Comets,[40] P. Constantin,[21,31] M. Csanád,[13] T. Csörgő,[25] T. Dahms,[50] K. Das,[15] G. David,[3] M.B. Deaton,[1] K. Dehmelt,[14] H. Delagrange,[51] A. Denisov,[18] D. d'Enterria,[9] A. Deshpande,[44,50] E.J. Desmond,[3] O. Dietzsch,[47] A. Dion,[50] M. Donadelli,[47] J.L. Drachenberg,[1] O. Drapier,[29] A. Drees,[50] A.K. Dubey,[57] A. Durum,[18] V. Dzhordzhadze,[4,52] Y.V. Efremenko,[39] J. Egdemir,[50] F. Ellinghaus,[8] W.S. Emam,[4] A. Enokizono,[17,30] H. En'yo,[43,44] B. Espagnon,[40] S. Esumi,[54] K.O. Eyser,[4] D.E. Fields,[37,44] M. Finger,[5,22] M. Finger, Jr.,[5,22] F. Fleuret,[29] S.L. Fokin,[27] B. Forestier,[32] Z. Fraenkel,[57] J.E. Frantz,[9,50] A. Franz,[3] A.D. Frawley,[15] K. Fujiwara,[43] Y. Fukao,[28,43] S.-Y. Fung,[4] T. Fusayasu,[36] S. Gadrat,[32] I. Garishvili,[52] F. Gastineau,[51] M. Germain,[51] A. Glenn,[8,52] H. Gong,[50] M. Gonin,[29] J. Gosset,[11] Y. Goto,[43,44] R. Granier de Cassagnac,[29] N. Grau,[21] S.V. Greene,[55] M. Grosse Perdekamp,[19,44] T. Gunji,[7] H.-Å. Gustafsson,[33] T. Hachiya,[17,43] A. Hadj Henni,[51] C. Haegemann,[37] J.S. Haggerty,[3] M.N. Hagiwara,[1] H. Hamagaki,[7] R. Han,[41] H. Harada,[17] E.P. Hartouni,[30] K. Haruna,[17] M. Harvey,[3] E. Haslum,[33] K. Hasuko,[43] R. Hayano,[7] M. Heffner,[30] T.K. Hemmick,[50] T. Hester,[4] J.M. Heuser,[43] X. He,[16] H. Hiejima,[19] J.C. Hill,[21] R. Hobbs,[37] M. Hohlmann,[14] M. Holmes,[55] W. Holzmann,[49] K. Homma,[17] B. Hong,[26] T. Horaguchi,[43,53] D. Hornback,[52] M.G. Hur,[23] T. Ichihara,[43,44] K. Imai,[28,43] J. Imrek,[12] M. Inaba,[54] Y. Inoue,[45,43] D. Isenhower,[1] L. Isenhower,[1] M. Ishihara,[43] T. Isobe,[7] M. Issah,[49] A. Isupov,[22] B.V. Jacak,[50,†] J. Jia,[9] J. Jin,[9] O. Jinnouchi,[44] B.M. Johnson,[3] K.S. Joo,[35] D. Jouan,[40] F. Kajihara,[7,43] S. Kametani,[7,56] N. Kamihara,[43,53] J. Kamin,[50] M. Kaneta,[44] J.H. Kang,[58] H. Kanou,[43,53] T. Kawagishi,[54] D. Kawall,[44] A.V. Kazantsev,[27] S. Kelly,[8] A. Khanzadeev,[42] J. Kikuchi,[56] D.H. Kim,[35] D.J. Kim,[58] E. Kim,[48] Y.-S. Kim,[23] E. Kinney,[8] A. Kiss,[13] E. Kistenev,[3] A. Kiyomichi,[43] J. Klay,[30] C. Klein-Boesing,[34] L. Kochenda,[42] V. Kochetkov,[18] B. Komkov,[42] M. Konno,[54] D. Kotchetkov,[4] A. Kozlov,[57] A. Král,[10] A. Kravitz,[9] P.J. Kroon,[3] J. Kubart,[5,20] G.J. Kunde,[31] N. Kurihara,[7] K. Kurita,[45,43] M.J. Kweon,[26] Y. Kwon,[52,58] G.S. Kyle,[38] R. Lacey,[49] Y.-S. Lai,[9] J.G. Lajoie,[21] A. Lebedev,[21] Y. Le Bornec,[40] S. Leckey,[50] D.M. Lee,[31] M.K. Lee,[58] T. Lee,[48] M.J. Leitch,[31] M.A.L. Leite,[47] B. Lenzi,[47] H. Lim,[48] T. Liška,[10] A. Litvinenko,[22] M.X. Liu,[31] X. Li,[6] X.H. Li,[4] B. Love,[55] D. Lynch,[3] C.F. Maguire,[55] Y.I. Makdisi,[3] A. Malakhov,[22] M.D. Malik,[37] V.I. Manko,[27] Y. Mao,[41,43] L. Mašek,[5,20] H. Masui,[54] F. Matathias,[9,50] M.C. McCain,[19] M. McCumber,[50] P.L. McGaughey,[31] Y. Miake,[54] P. Mikeš,[5,20] K. Miki,[54] T.E. Miller,[55] A. Milov,[50] S. Mioduszewski,[3] G.C. Mishra,[16] M. Mishra,[2] J.T. Mitchell,[3] M. Mitrovski,[49] A. Morreale,[4] D.P. Morrison,[3] J.M. Moss,[31] T.V. Moukhanova,[27] D. Mukhopadhyay,[55] J. Murata,[45,43] S. Nagamiya,[24] Y. Nagata,[54] J.L. Nagle,[8] M. Naglis,[57] I. Nakagawa,[43,44] Y. Nakamiya,[17] T. Nakamura,[17] K. Nakano,[43,53] J. Newby,[30] M. Nguyen,[50] B.E. Norman,[31] A.S. Nyanin,[27] J. Nystrand,[33] E. O'Brien,[3] S.X. Oda,[7] C.A. Ogilvie,[21] H. Ohnishi,[43] I.D. Ojha,[55] H. Okada,[28,43] K. Okada,[44] M. Oka,[54] O.O. Omiwade,[1] A. Oskarsson,[33] I. Otterlund,[33] M. Ouchida,[17] K. Ozawa,[7] R. Pak,[3] D. Pal,[55] A.P.T. Palounek,[31] V. Pantuev,[50] V. Papavassiliou,[38] J. Park,[48] W.J. Park,[26] S.F. Pate,[38] H. Pei,[21] J.-C. Peng,[19] H. Pereira,[11] V. Peresedov,[22] D.Yu. Peressounko,[27] C. Pinkenburg,[3] R.P. Pisani,[3] M.L. Purschke,[3] A.K. Purwar,[31,50] H. Qu,[16] J. Rak,[21,37] A. Rakotozafindrabe,[29] I. Ravinovich,[57] K.F. Read,[39,52] S. Rembeczki,[14] M. Reuter,[50] K. Reygers,[34] V. Riabov,[42] Y. Riabov,[42] G. Roche,[32] A. Romana,[29,*] M. Rosati,[21] S.S.E. Rosendahl,[33] P. Rosnet,[32] P. Rukoyatkin,[22] V.L. Rykov,[43] S.S. Ryu,[58] B. Sahlmueller,[34] N. Saito,[28,43,44] T. Sakaguchi,[3,7,56] S. Sakai,[54] H. Sakata,[17] V. Samsonov,[42] H.D. Sato,[28,43] S. Sato,[3,24,54] S. Sawada,[24] J. Seele,[8] R. Seidl,[19] V. Semenov,[18] R. Seto,[4] D. Sharma,[57] T.K. Shea,[3] I. Shein,[18] A. Shevel,[42,49] T.-A. Shibata,[43,53] K. Shigaki,[17] M. Shimomura,[54] T. Shohjoh,[54] K. Shoji,[28,43] A. Sickles,[50] C.L. Silva,[47] D. Silvermyr,[39] C. Silvestre,[11] K.S. Sim,[26] C.P. Singh,[2] V. Singh,[2] S. Skutnik,[21] M. Slunečka,[5,22] W.C. Smith,[1] A. Soldatov,[18] R.A. Soltz,[30] W.E. Sondheim,[31] S.P. Sorensen,[52] I.V. Sourikova,[3] F. Staley,[11] P.W. Stankus,[39] E. Stenlund,[33] M. Stepanov,[38] A. Ster,[25]

S.P. Stoll,[3] T. Sugitate,[17] C. Suire,[40] J.P. Sullivan,[31] J. Sziklai,[25] T. Tabaru,[44] S. Takagi,[54] E.M. Takagui,[47] A. Taketani,[43,44] K.H. Tanaka,[24] Y. Tanaka,[36] K. Tanida,[43,44] M.J. Tannenbaum,[3] A. Taranenko,[49] P. Tarján,[12] T.L. Thomas,[37] M. Togawa,[28,43] A. Toia,[50] J. Tojo,[43] L. Tomášek,[20] H. Torii,[43] R.S. Towell,[1] V-N. Tram,[29] I. Tserruya,[57] Y. Tsuchimoto,[17,43] S.K. Tuli,[2] H. Tydesjö,[33] N. Tyurin,[18] C. Vale,[21] H. Valle,[55] H.W. van Hecke,[31] J. Velkovska,[55] R. Vertesi,[12] A.A. Vinogradov,[27] M. Virius,[10] V. Vrba,[20] E. Vznuzdaev,[42] M. Wagner,[28,43] D. Walker,[50] X.R. Wang,[38] Y. Watanabe,[43,44] J. Wessels,[34] S.N. White,[3] N. Willis,[40] D. Winter,[9] C.L. Woody,[3] M. Wysocki,[8] W. Xie,[4,44] Y.L. Yamaguchi,[56] A. Yanovich,[18] Z. Yasin,[4] J. Ying,[16] S. Yokkaichi,[43,44] G.R. Young,[39] I. Younus,[37] I.E. Yushmanov,[27] W.A. Zajc,[9] O. Zaudtke,[34] C. Zhang,[9,39] S. Zhou,[6] J. Zimányi,[25,*] and L. Zolin[22]

(PHENIX Collaboration)

[1]*Abilene Christian University, Abilene, TX 79699, USA*
[2]*Department of Physics, Banaras Hindu University, Varanasi 221005, India*
[3]*Brookhaven National Laboratory, Upton, NY 11973-5000, USA*
[4]*University of California - Riverside, Riverside, CA 92521, USA*
[5]*Charles University, Ovocný trh 5, Praha 1, 116 36, Prague, Czech Republic*
[6]*China Institute of Atomic Energy (CIAE), Beijing, People's Republic of China*
[7]*Center for Nuclear Study, Graduate School of Science, University of Tokyo, 7-3-1 Hongo, Bunkyo, Tokyo 113-0033, Japan*
[8]*University of Colorado, Boulder, CO 80309, USA*
[9]*Columbia University, New York, NY 10027 and Nevis Laboratories, Irvington, NY 10533, USA*
[10]*Czech Technical University, Zikova 4, 166 36 Prague 6, Czech Republic*
[11]*Dapnia, CEA Saclay, F-91191, Gif-sur-Yvette, France*
[12]*Debrecen University, H-4010 Debrecen, Egyetem tér 1, Hungary*
[13]*ELTE, Eötvös Loránd University, H - 1117 Budapest, Pázmány P. s. 1/A, Hungary*
[14]*Florida Institute of Technology, Melbourne, FL 32901, USA*
[15]*Florida State University, Tallahassee, FL 32306, USA*
[16]*Georgia State University, Atlanta, GA 30303, USA*
[17]*Hiroshima University, Kagamiyama, Higashi-Hiroshima 739-8526, Japan*
[18]*IHEP Protvino, State Research Center of Russian Federation, Institute for High Energy Physics, Protvino, 142281, Russia*
[19]*University of Illinois at Urbana-Champaign, Urbana, IL 61801, USA*
[20]*Institute of Physics, Academy of Sciences of the Czech Republic, Na Slovance 2, 182 21 Prague 8, Czech Republic*
[21]*Iowa State University, Ames, IA 50011, USA*
[22]*Joint Institute for Nuclear Research, 141980 Dubna, Moscow Region, Russia*
[23]*KAERI, Cyclotron Application Laboratory, Seoul, Korea*
[24]*KEK, High Energy Accelerator Research Organization, Tsukuba, Ibaraki 305-0801, Japan*
[25]*KFKI Research Institute for Particle and Nuclear Physics of the Hungarian Academy of Sciences (MTA KFKI RMKI), H-1525 Budapest 114, POBox 49, Budapest, Hungary*
[26]*Korea University, Seoul, 136-701, Korea*
[27]*Russian Research Center "Kurchatov Institute", Moscow, Russia*
[28]*Kyoto University, Kyoto 606-8502, Japan*
[29]*Laboratoire Leprince-Ringuet, Ecole Polytechnique, CNRS-IN2P3, Route de Saclay, F-91128, Palaiseau, France*
[30]*Lawrence Livermore National Laboratory, Livermore, CA 94550, USA*
[31]*Los Alamos National Laboratory, Los Alamos, NM 87545, USA*
[32]*LPC, Université Blaise Pascal, CNRS-IN2P3, Clermont-Fd, 63177 Aubiere Cedex, France*
[33]*Department of Physics, Lund University, Box 118, SE-221 00 Lund, Sweden*
[34]*Institut für Kernphysik, University of Muenster, D-48149 Muenster, Germany*
[35]*Myongji University, Yongin, Kyonggido 449-728, Korea*
[36]*Nagasaki Institute of Applied Science, Nagasaki-shi, Nagasaki 851-0193, Japan*
[37]*University of New Mexico, Albuquerque, NM 87131, USA*
[38]*New Mexico State University, Las Cruces, NM 88003, USA*
[39]*Oak Ridge National Laboratory, Oak Ridge, TN 37831, USA*
[40]*IPN-Orsay, Universite Paris Sud, CNRS-IN2P3, BP1, F-91406, Orsay, France*
[41]*Peking University, Beijing, People's Republic of China*
[42]*PNPI, Petersburg Nuclear Physics Institute, Gatchina, Leningrad region, 188300, Russia*
[43]*RIKEN, The Institute of Physical and Chemical Research, Wako, Saitama 351-0198, Japan*
[44]*RIKEN BNL Research Center, Brookhaven National Laboratory, Upton, NY 11973-5000, USA*
[45]*Physics Department, Rikkyo University, 3-34-1 Nishi-Ikebukuro, Toshima, Tokyo 171-8501, Japan*
[46]*Saint Petersburg State Polytechnic University, St. Petersburg, Russia*
[47]*Universidade de São Paulo, Instituto de Física, Caixa Postal 66318, São Paulo CEP05315-970, Brazil*
[48]*System Electronics Laboratory, Seoul National University, Seoul, Korea*
[49]*Chemistry Department, Stony Brook University, Stony Brook, SUNY, NY 11794-3400, USA*
[50]*Department of Physics and Astronomy, Stony Brook University, SUNY, Stony Brook, NY 11794, USA*
[51]*SUBATECH (Ecole des Mines de Nantes, CNRS-IN2P3, Université de Nantes) BP 20722 - 44307, Nantes, France*

[52] University of Tennessee, Knoxville, TN 37996, USA
[53] Department of Physics, Tokyo Institute of Technology, Oh-okayama, Meguro, Tokyo 152-8551, Japan
[54] Institute of Physics, University of Tsukuba, Tsukuba, Ibaraki 305, Japan
[55] Vanderbilt University, Nashville, TN 37235, USA
[56] Waseda University, Advanced Research Institute for Science and Engineering, 17 Kikui-cho, Shinjuku-ku, Tokyo 162-0044, Japan
[57] Weizmann Institute, Rehovot 76100, Israel
[58] Yonsei University, IPAP, Seoul 120-749, Korea
(Dated: February 15, 2013)

For Au+Au collisions at 200 GeV we measure neutral pion production with good statistics for transverse momentum, $p_{\rm T}$, up to 20 GeV/c. A fivefold suppression is found, which is essentially constant for $5<p_{\rm T}<20$ GeV/c. Experimental uncertainties are small enough to constrain any model-dependent parameterization for the transport coefficient of the medium, e.g. $\langle\hat{q}\rangle$ in the parton quenching model. The spectral shape is similar for all collision classes, and the suppression does not saturate in Au+Au collisions; instead, it increases proportional to the number of participating nucleons, as ${N_{\rm part}}^{2/3}$.

PACS numbers: 25.75.Dw

Large transverse momentum ($p_{\rm T}$) hadrons originate primarily from the fragmentation of hard scattered quarks or gluons. In high energy p+p collisions this is well described in the framework of perturbative QCD [1]. In ultra-relativistic heavy ion collisions such hard scatterings occur in the early phase of the reaction, and the transiting partons serve as probes of the strongly interacting medium produced in the collisions. Lattice QCD predicts a phase transition to a plasma of deconfined quarks and gluons, which induces gluon radiation from the scattered parton and depletes hadron production at high $p_{\rm T}$ ("jet quenching") [2, 3]. The measurements in Au+Au collisions at RHIC showed suppressed hadron yields in central collisions [4] as predicted [5, 6], and motivated an advanced theoretical study of radiative energy loss using different approaches [7].

All the energy loss models must incorporate space-time evolution of the medium, as it is not static, as well as the initial distribution of the partons throughout the medium. Models generally also include an input parameter for the medium density and/or the coupling. Different assumptions in the various models lead to similar descriptions of the π^0 suppression with different model-dependent parameters [8, 9]. For instance, the Parton Quenching model (PQM) is a Monte Carlo using the quenching weights from BDMPS [5] that combines the coupling strength with the color-charge density to create a single transport coefficient, often referred to as $\langle\hat{q}\rangle$ [10, 11], which gives the average squared transverse momentum transferred from the medium to the parton per mean free path.

Measurement of identified particles up to the highest possible $p_{\rm T}$, establishing the magnitude, $p_{\rm T}$ and centrality dependence of the suppression pattern, is crucial to constrain the theoretical models and separate contributions of initial and final state effects from the energy loss mechanism. Collision centrality is related to the average pathlength of the parton in the medium. The suppression of π^0 puts important constraints on calculations of the energy loss, as neutral pions can be identified up to very high $p_{\rm T}$. Whereas it has also been shown that the di-hadron suppression at high $p_{\rm T}$ may be somewhat more sensitive than single hadron suppression to the medium opacity [12], such improvement is contingent upon the theoretical and experimental, statistical and systematic uncertainties.

This Letter reports on the measurement of neutral pions up to $p_{\rm T}$=20 GeV/c in Au+Au collisions at $\sqrt{s_{NN}}$=200 GeV at RHIC, using the high statistics collected in Run-4. Based upon the data we extract the $\langle\hat{q}\rangle$ parameter of the PQM model for the most central collisions.

The analysis used 1.03×10^9 minimum bias events taken by the PHENIX experiment [13]. Collision centrality was determined from the correlation between the number of charged particles detected in the Beam-Beam Counters (BBC, $3.0<|\eta|<3.9$) and the energy measured in the Zero Degree Calorimeters (ZDC). A Glauber model Monte Carlo with a simulation of the BBC and ZDC responses was used to estimate the associated average number of participating nucleons ($\langle N_{\rm part}\rangle$) and binary nucleon-nucleon collisions ($\langle N_{\rm coll}\rangle$) for each centrality bin [14].

Neutral pions were measured in the $\pi^0 \rightarrow \gamma\gamma$ decay channel with the photons reconstructed in the Electromagnetic Calorimeter (EMCal) located in the two central arms of PHENIX ($|\eta| \leq 0.35$). The EMCal [15] consists of two subsystems: six sectors of lead-scintillator sandwich calorimeter (PbSc) and two sectors of lead-glass Čerenkov calorimeter (PbGl) at the radial distance of about 5 m. The fine segmentation of the EMCal ($\delta\phi \times \delta\eta \sim 0.01 \times 0.01$ for PbSc and $\sim 0.008 \times 0.008$ for PbGl) ensures that the two photons from a $\pi^0 \rightarrow \gamma\gamma$ decay are well resolved up to $p_{\rm T}^{\pi^0} \approx 12$ (PbSc) and 16 (PbGl) GeV/c. Data from the two subsystems were analyzed separately and the fully corrected results were combined.

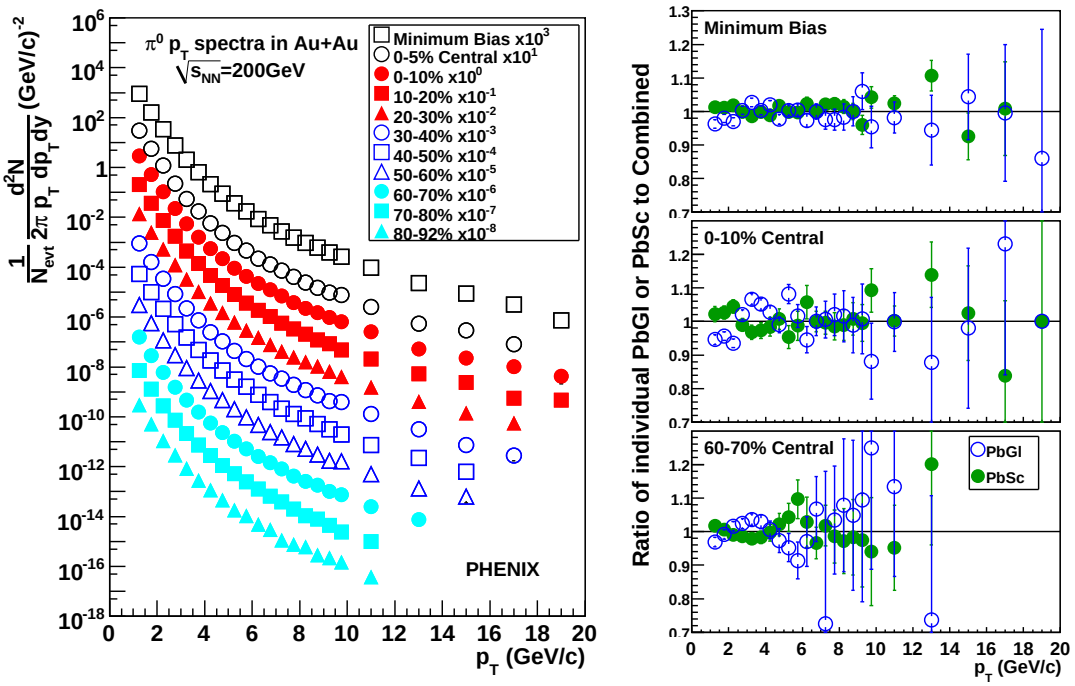

FIG. 1: Left: π^0 invariant yields for different centralities (PbSc and PbGl combined). Right: consistency between the results obtained separately from PbSc and PbGl

Details of the analysis including extraction of the raw π^0 yield, correction for acceptance, detector response (energy resolution, dead areas), reconstruction efficiency (particle identification cuts) have been described elsewhere [16, 17]. In this analysis the higher p_T range required correction for losses in the observed (raw) π^0s due to "cluster merging".

With increasing π^0 momentum, the minimum opening angle of the two decay photons decreases, and eventually they will be reconstructed as a single cluster. Such "merging" reaches 50% of the total raw yield at p_T=14 GeV/c in the PbSc and at p_T=18 GeV/c in the PbGl due to their different granularity and Molìradius. Merged clusters were rejected by various shower profile cuts, and the loss was determined by simulated single π^0s embedded into real events and analyzed with the same cuts. The loss increases slowly with centrality. The systematic uncertainties were estimated by comparing π^0 yields in the PbSc extracted in different windows of asymmetry $|E_{\gamma_1} - E_{\gamma_2}|/(E_{\gamma_1} + E_{\gamma_2})$ and also by comparing yields in the PbSc and PbGl.

We considered two sources of π^0s not originating from the collision vertex: those produced in nuclear interactions of hadrons with detector material (instrumental background) and feed-down products from weak decay of higher mass hadrons (physics background). Based upon simulations both the instrumental background and feed-down background were found to be negligible (<1% above p_T>2.0 GeV/c) except for the contribution from K^0_S decay (≈3% of π^0 yield for p_T>1 GeV/c), which has been subtracted from the data. Finally the yields were corrected to the center of the p_T bins using the local slope.

TABLE I: Summary of the systematic uncertainties on the π^0 yield extracted independently with the PbSc (PbGl) electromagnetic calorimeters. All but one, off-vertex π^0, are uncorrelated between PbSc and PbGl, and centrality dependence is negligible. The last row is the total systematic uncertainty on the combined spectra. Detailed description of how the errors are correlated as a function of p_T can be found in [17].

p_T (GeV/c)	2	6	10	16
uncertainty source	PbSc (PbGl)			
yield extraction (%)	3.0 (4.1)	3.0 (4.1)	3.0 (4.1)	3.0 (4.1)
PID efficiency (%)	3.5 (3.9)	3.5 (3.5)	3.5 (3.7)	3.5 (3.9)
Energy scale (%)	6.7 (9.0)	8.0 (9.2)	8.0 (8.2)	8.0 (12.3)
Acceptance (%)	1.5 (4.1)	1.5 (4.1)	1.5 (4.1)	1.5 (4.1)
π^0 merging (%)	– (–)	– (–)	4.4 (–)	28 (4.8)
Conversion (%)	3.0 (2.5)	3.0 (2.5)	3.0 (2.5)	3.0 (2.5)
off-vertex π^0 (%)	1.5 (1.5)	1.5 (1.5)	1.5 (1.5)	1.5 (1.5)
Total (%)	8.7 (12)	9.8 (11)	11 (11)	30 (15)
PbSc and PbGl combined: Total (%)	7.0	7.5	7.6	14

The main sources of systematic uncertainties are yield extraction, efficiency corrections, and energy scale, none of which exhibit a significant centrality dependence. The PbSc and PbGl detectors have quite different systematics with all but one of them (off-vertex π^0) uncorrelated.

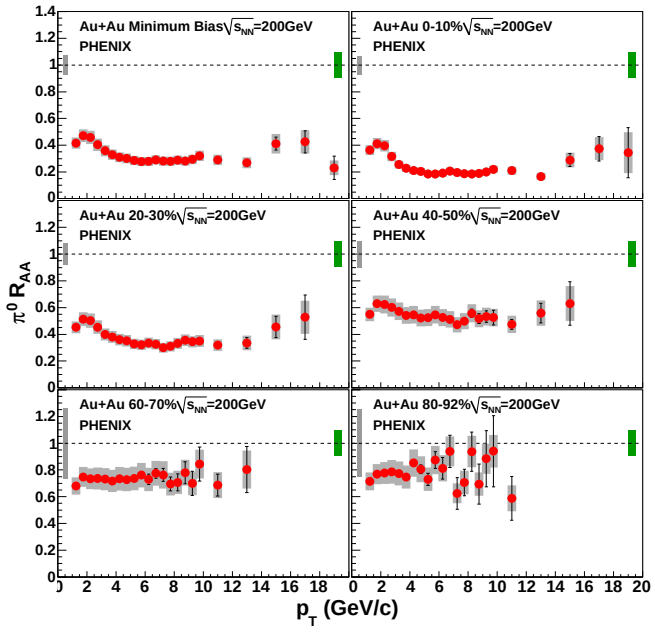

FIG. 2: Nuclear modification factor ($R_{\rm AA}$) for π^0s. Error bars are statistical and $p_{\rm T}$-uncorrelated errors, boxes around the points indicate $p_{\rm T}$-correlated errors. Single box around $R_{\rm AA}$=1 on the left is the error due to $N_{\rm coll}$, whereas the single box on the right is the overall normalization error of the p+p reference spectrum.

Therefore, when combining their results, the total error is reduced in the weighted average of the two independent measurements. The final systematic uncertainties (one standard deviation) on the spectra are shown in Table I.

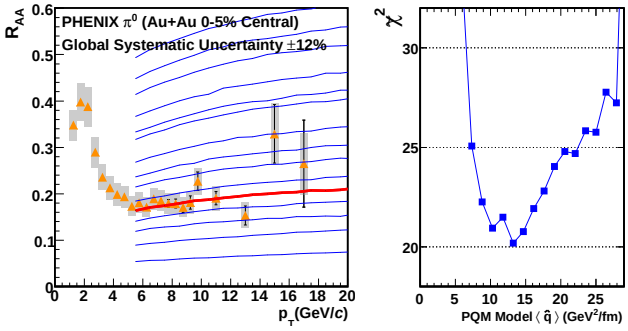

FIG. 3: Left: π^0 $R_{\rm AA}$ for the most central (0-5%) Au+Au collisions and PQM model calculations for different values of $\langle\hat{q}\rangle$. Red curve: best fit. Right: $\tilde{\chi}^2(\epsilon_b, \epsilon_c, p)$ distribution for a wide range of values of $\langle\hat{q}\rangle$.

The left panel of Figure 1 shows the π^0 invariant yield spectra for all centralities as well as minimum bias, combined from the independent PbSc and PbGl measurements. In the overlap region the results are consistent with those published earlier [16] while the errors are reduced by a factor of 2 to 2.5. The right panel shows the ratios of PbSc and PbGl spectra to the combined

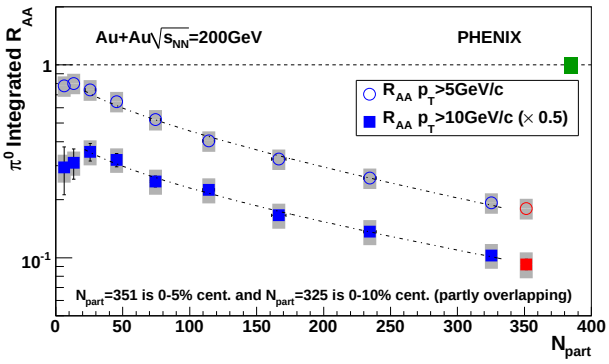

FIG. 4: Integrated nuclear modification factor ($R_{\rm AA}$) for π^0 as a function of collision centrality expressed in terms of $N_{\rm part}$. The error bars/bands are the same as in Fig. 2. The last two points correspond to overlapping centrality bins, 0-10% and 0-5%. The dashed lines show the fit to a function. See text.

one at three centralities. The spectra are quite similar at all centralities: when fitting $p_{\rm T}$>5 GeV/c with a power law function ($\propto p_{\rm T}^n$), the exponents vary from $n = -8.00 \pm 0.12$ in 0-5% to $n = -8.06 \pm 0.08$ in the 80-92% (most peripheral) bin. Note that $n = -8.22 \pm 0.09$ in p+p collisions. The errors are combined statistical errors and systematic uncertainties.

To quantify the comparison of spectra in heavy ion and p+p collisions, the nuclear modification factor ($R_{\rm AA}$)

$$R_{\rm AA} = \frac{1/N_{\rm evt} dN/dydp_{\rm T}}{\langle T_{\rm AB}\rangle\, d\sigma_{pp}/dydp_{\rm T}}$$

is used where σ_{pp} is the production cross section of the particle in p+p collisions, and $\langle T_{\rm AB}\rangle$ is the nuclear thickness function averaged over a range of impact parameters for the given centrality, calculated within a Glauber model [14]. Figure 2 shows $R_{\rm AA}$ for π^0 at different centralities, the 0-5% bin is shown on Figure 3. The reference p+p yield was obtained from the 2005 (Run-5) RHIC p+p measurement [18].

$R_{\rm AA}$ reaches ~0.2 in 0-10 % centrality at $p_{\rm T}$>5 GeV/c with very little (if any) $p_{\rm T}$ dependence. This trend is compatible with most current energy loss models but not with a semi-opaque medium assumption, where $R_{\rm AA}$ would decrease with increasing $p_{\rm T}$ [8]. While its magnitude changes, the suppression pattern itself is remarkably similar at all centralities suggesting that the bulk $R_{\rm AA}$ (integrated over the azimuthal angle) is sensitive only to the $N_{\rm part}$ but not to the specific geometry. Consequently, study of the $p_{\rm T}$-integrated $R_{\rm AA}$ *vs.* centrality is instructive.

Figure 4 shows the integrated nuclear modification factor ($p_{\rm T}$>5 GeV/c, and $p_{\rm T}$>10 GeV/c) for π^0s as a function of centrality, with the last two points indicating overlapping 0-10% and 0-5% bins. In both cases the suppression increases monotonically with $N_{\rm part}$ without any sign of saturation, suggesting that larger colliding sys-

tems (such as U+U planned at RHIC) should exhibit even more suppression.

The common power-law behavior ($\propto p_{\rm T}^n$) in p+p and Au+Au allows the suppression to be re-interpreted as a fractional energy loss $S_{\rm loss} = 1 - R_{\rm AA}^{1/(n-2)}$ where n is the power-law exponent, and we found that $S_{\rm loss} \propto N_{\rm part}^a$ [16]. Fitting the integrated $R_{\rm AA}$ with a function $R_{\rm AA} = (1 - S_0 N_{\rm part}^a)^{n-2}$ gives $a = 0.58 \pm 0.07$ for $N_{\rm part}$>20 for $p_{\rm T}$>5 GeV/c, and $a = 0.56 \pm 0.10$ for $p_{\rm T}$>10 GeV/c. The GLV [6] and PQM [11] models predict that $a \approx 2/3$, which is consistent with the data. The fitted values of S_0 are $(8.3\pm3.3)\times10^{-3}$ and $(9.2\pm4.9)\times10^{-3}$ for $p_{\rm T}$>5 GeV/c and $p_{\rm T}$>10 GeV/c, respectively. The fits are shown as dashed lines in Fig. 4. Note that in this interpretation a constant $S_{\rm loss}$ (independent of $p_{\rm T}$) implies that the energy loss increases with $p_{\rm T}$.

We use the highest centrality (0–5%) $R_{\rm AA}$ data as shown on Fig. 3 to constrain the PQM model parameters. The procedure is described in detail in [17]. First we break up the errors of the measured points into Type A ($p_{\rm T}$-uncorrelated, statistical $\oplus$ systematic, σ_i), Type B ($p_{\rm T}$-correlated, σ_{b_i}, boxes on Fig. 2) and Type C (normalization, uniform fractional shift for all points, σ_c). Then taking the theory curves calculated for different values of the input parameter p, one would normally perform a least-squares fit to the theory by finding the values of p, ϵ_b, ϵ_c that minimize:

$$\chi^2 = \left[\sum_{i=1}^{n} \frac{(y_i + \epsilon_b\sigma_{b_i} + \epsilon_c y_i \sigma_c - \mu_i(p))^2}{\sigma_i^2} + \epsilon_b^2 + \epsilon_c^2\right] \quad , \tag{1}$$

where ϵ_b and ϵ_c are the fractions of the type B and C systematic uncertainties that all points are displaced together. It is important to note that Eq. 1 follows the χ^2-distribution with $n+2$ degrees of freedom when p, ϵ_b and ϵ_c are fixed, because it is the sum of $n+2$ independent Gaussian distributed random variables.

However, for the present data, the statistical and random systematic uncertainties are such that the shift in the measurement y_i due to the correlated systematic uncertainties preserves the fractional type A uncertainty. Thus, we use a least squares fit of the quantity $\tilde{\chi}^2$ to estimate the best fit parameters, where $\tilde{\chi}^2$ is Eq. 1 with σ_i replaced by $\tilde{\sigma}_i = \sigma_i(y_i + \epsilon_b\sigma_{b_i} + \epsilon_c y_i\sigma_c)/y_i$, which is the uncertainty scaled by the multiplicative shift in y_i such that the fractional uncertainty is unchanged under shifts. For any fixed values of ϵ_b, ϵ_c, $\tilde{\chi}^2$ still follows the χ^2 distribution with $n+2$ degrees of freedom. The best fit, the minimum of $\tilde{\chi}^2$, is found by standard methods (for example using a MINUIT type minimization algorithm) and the correlated uncertainties of the best fit parameters are estimated in the Gaussian approximation by $\tilde{\chi}^2(\epsilon_b, \epsilon_c, p) = \tilde{\chi}^2_{\rm min} + N^2$ for N standard deviation uncertainties. The right panel of Fig. 4 shows the $\tilde{\chi}^2(\epsilon_b, \epsilon_c, p)$ distribution for a wide range of values of the PQM model parameter $\langle\hat{q}\rangle$. Our data constrain the PQM model transport coefficient $\langle\hat{q}\rangle$ as $13.2\ ^{+2.1}_{-3.2}$ and $^{+6.3}_{-5.2}$ GeV^2/fm at the one and two standard deviation levels. These constraints include only the experimental uncertainties and do not account for the large model dependent differences in the quenching scenario and description of the medium. Extracting fundamental model-independent properties of the medium from the present data requires resolution of ambiguities and open questions in the models themselves which also will have to account simultaneously for the $p_{\rm T}$ and centrality (average pathlength) dependence. This work demonstrates the power of data for pion production in constraining the energy loss of partons. The data can be fitted with a constant in the entire $p_{\rm T}>5$ GeV/c range as well: the slope of a simple linear fit is $0.0017\ ^{+0.0035}_{-0.0039}$ and $^{+0.0070}_{-0.0076}$ c/GeV at the one and two standard deviation levels.

In summary, PHENIX has measured neutral pions in Au+Au collisions at $\sqrt{s_{NN}}$=200 GeV at mid rapidity in the transverse momentum range of 1<$p_{\rm T}$<20 GeV/c, analyzing high statistics RHIC Run-4 run data. The shape of the spectra is similar for all centralities, as is the shape of $R_{\rm AA}(p_{\rm T})$ at $p_{\rm T}$>5GeV/c. In central collisions the yield is suppressed by a factor of ∼5 at 5 GeV/c compared to the binary scaled p+p reference and the suppression prevails with little or no change up to 20 GeV/c. Studying the integrated $R_{\rm AA}$ *vs.* centrality we find that it does not saturate at this nuclear size; also the prediction $S_{\rm loss} \propto N_{\rm part}^{2/3}$[6, 11] is consistent with our data and in this picture the energy loss increases with $p_{\rm T}$. Using the 0-5% (most central) $R_{\rm AA}$ we find that the transport coefficient $\langle\hat{q}\rangle$ of the PQM model is constrained to $13.2\ ^{+2.1}_{-3.2}$ $(^{+6.3}_{-5.2})$ GeV^2/fm at the one (two) σ level. A simple linear fit with zero slope is also consistent with our data.

We thank the staff of the Collider-Accelerator and Physics Departments at BNL for their vital contributions. We acknowledge support from the Office of Nuclear Physics in DOE Office of Science and NSF (U.S.A.), MEXT and JSPS (Japan), CNPq and FAPESP (Brazil), NSFC (China), MSMT (Czech Republic), IN2P3/CNRS, and CEA (France), BMBF, DAAD, and AvH (Germany), OTKA (Hungary), DAE (India), ISF (Israel), KRF and KOSEF (Korea), MES, RAS, and FAAE (Russia), VR and KAW (Sweden), U.S. CRDF for the FSU, US-Hungarian NSF-OTKA-MTA, and US-Israel BSF.

* Deceased
† PHENIX Spokesperson: jacak@skipper.physics.sunysb.edu

[1] D. de Florian and W. Vogelsang, Phys. Rev. **D71**, 114004 (2005).
[2] M. Gyulassy and M. Plumer, Phys. Lett. **B243**, 432 (1990).
[3] X.-N. Wang and M. Gyulassy, Phys. Rev. Lett. **68**, 1480 (1992).
[4] K. Adcox et al., Phys. Rev. Lett. **88**, 022301 (2002).

[5] R. Baier, Y. L. Dokshitzer, A. H. Mueller, S. Peigne, and D. Schiff, Nucl. Phys. **B484**, 265 (1997).
[6] M. Gyulassy, P. Levai, and I. Vitev, Phys. Rev. Lett. **85**, 5535 (2000).
[7] P. Arnold, G. D. Moore, and L. G. Yaffe, JHEP **06**, 030 (2002).
[8] T. Renk, Phys. Rev. **C74**, 034906 (2006).
[9] R. Baier and D. Schiff, JHEP **09**, 059 (2006).
[10] A. Dainese, C. Loizides, and G. Paic, Eur. Phys. J. **C38**, 461 (2005).
[11] C. Loizides, Eur. Phys. J. **C49**, 339 (2007).
[12] H. Zhang, J. F. Owens, E. Wang, and X.-N. Wang, Phys. Rev. Lett. **98**, 212301 (2007).
[13] K. Adcox et al., Nucl. Instrum. Meth. **A499**, 469 (2003).
[14] M. L. Miller, K. Reygers, S. J. Sanders, and P. Steinberg, Annu. Rev. Nucl. Part. Sci. **57**, 205 (2007).
[15] L. Aphecetche et al., Nucl. Instrum. Meth. **A499**, 521 (2003).
[16] S. S. Adler et al., Phys. Rev. **C76**, 034904 (2007).
[17] S. S. Adler et al., arXiv:0801.1665 [nucl-ex].
[18] A. Adare, Phys. Rev. **D76**, 051106 (2007).